Salicylate suppresses the oncogenic hyaluronan network in metastatic breast cancer cells

Theodoros T. Karalis[a], **Athanasios Chatzopoulos**[a], **Aikaterini Kondyli**[a], **Alexios J. Aletras**[a], **Nikos K. Karamanos**[a], **Paraskevi Heldin**[b] and **Spyros S. Skandalis**[a]

a - Biochemistry, *Biochemical Analysis & Matrix Pathobiology Res. Group, Laboratory of Biochemistry, Department of Chemistry, University of Patras, 26110 Patras, Greece*
b - Department of Medical Biochemistry and Microbiology, *Uppsala University, Box 582, SE-751 23 Uppsala, Sweden*

Correspondence to Spyros S. Skandalis: *skandalis@upatras.gr.*
https://doi.org/10.1016/j.mbplus.2020.100031

Abstract

The oncogenic role of hyaluronan in several aspects of tumor biology has been well established. Recent studies by us and others suggest that inhibition of hyaluronan synthesis could represent an emerging therapeutic approach with significant clinical relevance in controlling different breast cancer subtypes, including triple-negative breast cancer. Epidemiological and preclinical studies have revealed the therapeutic potential of aspirin (acetyl salicylate), a classical anti-inflammatory drug, in patients with cancer. However, the underlying molecular mechanisms remain unknown. The present study demonstrates that salicylate, a break down product of aspirin in vivo, alters the organization of hyaluronan matrices by affecting the expression levels of hyaluronan synthesizing (HAS1, 2, 3) and degrading (HYAL-1, -2) enzymes, and that of hyaluronan receptor CD44. In particular, salicylate was found to potently activate AMPK, a kinase known to inhibit HAS2 activity, and caused a dose-dependent decrease of cell associated (intracellular and membrane-bound) as well as secreted hyaluronan, followed by the down-regulation of HAS2 and the induction of HYAL-2 and CD44 in metastatic breast cancer cells. These salicylate-mediated effects were associated with the redistribution of CD44 and actin cytoskeleton that resulted in a less motile cell phenotype. Interestingly, salicylate inhibited metastatic breast cancer cell proliferation and growth by inducing cell growth arrest without signs of apoptosis as evidenced by the substantial decrease of cyclin D1 protein and the absence of cleaved caspase-3, respectively. Collectively, our study offers a possible direction for the development of new matrix-based targeted treatments of metastatic breast cancer subtypes via inhibition of hyaluronan, a pro-angiogenic, pro-inflammatory and tumor promoting glycosaminoglycan.

Introduction

Breast cancer, the second leading cause of cancer deaths in women, exists in multiple subtypes including ER-positive (luminal A, luminal B) and ER-negative (HER2 positive, basal-like/triple negative) tumors according to gene expression patterns and molecular markers. Metastatic breast cancers (such as triple negative breast cancer, TNBC) have the worst prognosis due to lack of effective targeted therapies [1]. Therefore, there is an urgent need for new treatment schemes that can completely and selectively ablate metastatic breast cancers with little or no side effects.

Excessive amounts of hyaluronan due to deregulation of hyaluronan-synthesizing enzymes (mainly HAS2) are often correlated to poor outcome of patients with metastatic breast cancer (including TNBC) [2–4]. Hyaluronan, one of the principal constituents of the tumor microenvironment, is a linear glycosaminoglycan found predominately in the extra- and pericellular spaces of most animal tissues

[5,6], but it is also detected intracellularly under specific developmental and pathological conditions, including inflammation and cancer [7,8]. Hyaluronan interacts with specific proteins, like TSG6, and cell membrane receptors, like CD44, RHAMM, HARE and toll-like receptors (TLR) 2/4, which mediate its cellular effects [6,9–14]. Notably, hyaluronan and CD44 are prominent components of stem cell niches and their interactions play a critical role in the maintenance of cancer stem cell phenotype and the promotion of the metastatic potential of multiple types of cancer [15].

Hyaluronan is distinct from the other glycosaminoglycans in size and length, site of biosynthesis, and lack of core protein and sulfate esters [5,16]. The synthesis and degradation of hyaluronan are tightly regulated in a cell- and context-dependent manner [17,18]. Hyaluronan is synthesized by three plasma membrane integrated hyaluronan-synthesizing isoenzymes (HAS1, HAS2 and HAS3), which are controlled in multiple ways. Apart from their regulation at the transcriptional level as a response to growth factors [19] and a specific natural antisense transcript HAS2-AS [20], recent reports have demonstrated that HASs (in particular HAS2) are also subject to post-translational modifications that critically control their stability and activity [4,21–24]. Specifically, monoubiquitination at Lys^{190} and O-GlcNAcylation at Ser^{221} enhance the stability and enzymatic activity of HAS2 and thus stimulate hyaluronan synthesis [25,26]. In contrast, phosphorylation of HAS2 at Thr^{110}, a residue located on a cytosolic loop of the enzyme, by the adenosine monophosphate-activated protein kinase (AMPK) suppresses HAS2 enzymatic activity and hyaluronan production [27]. AMPK, a major cellular metabolic sensor and regulator, is a heterotrimeric kinase formed by a catalytic α subunit and two regulatory β and γ subunits [28]. In response to metabolic stress, AMPK is activated by phosphorylation at Thr^{172} in the α subunit and phosphorylates target proteins that switch on catabolic pathways generating ATP, while switching off ATP-consuming processes at the same time [29].

Numerous epidemiological and preclinical studies have shown that aspirin (acetyl salicylate), a widely used nonsteroidal anti-inflammatory drug (NSAID), exhibits anticancer effects, while recent clinical trials have revealed the potential of aspirin for cancer prevention and therapy [30–33]. Despite the wide appreciation of the beneficial effects of aspirin in patients with cancer, the underlying molecular mechanisms remain unclear. In vivo, aspirin is rapidly broken down to salicylate by endogenous esterases, which remove the acetyl group [34,35]. Accumulating evidence suggest that salicylate and aspirin can both exert anti-inflammatory functions by interfering with prostaglandin synthesis through inhibition of cyclooxygenases (COX) enzymes through, however, different mechanisms. For example, aspirin inhibits COX activity by acetylation, while salicylate blocks COX expression at the transcriptional level [36,37]. Recent studies have revealed additional targets of these compounds, such as histones [38], cell cycle regulators [39], heparanase [40], uPA [41], and AMPK [42].

The finding that salicylate can directly activate AMPK together with the inhibitory action of AMPK on hyaluronan synthesis through HAS2 phosphorylation and inactivation, led us to investigate whether hyaluronan could be a potential target of salicylate. Our findings suggest that salicylate inhibits the synthesis of hyaluronan through activation of AMPK and potently suppresses the aggressiveness of MDA-MB-231 cells, a widely used breast cancer cell model for metastatic TNBC subtype.

Results

Salicylate activates AMPK in breast cancer cells

It has been reported that salicylate activates AMPK in human embryonic kidney cells and this was associated with increased phosphorylation of Thr^{172} on AMPK [42]. To explore this possibility in breast cancer cells, MDA-MB-231 cells were subjected to a 24 h treatment with 10 mM salicylate in the absence or presence of fetal bovine serum (FBS, 10%). Indeed, the results showed that salicylate induced the phosphorylation of AMPK on Thr^{172} also in breast cancer cells under both culture conditions (Fig. 1A). In serum-cultured cells, phosphorylated AMPK was nearly undetectable or at low levels, while salicylate treatment resulted in a robust phosphorylation of AMPK at levels similar to those observed after incubation with AICAR (5-amino-1-β-D-ribofuranosyl-imidazole-4-carboxamide), an AMP analog that is known to stimulate AMPK activity (Fig. 1A). In addition, 4-methylumbelliferone (4-MU), an established inhibitor of hyaluronan synthesis, also induced AMPK phosphorylation in serum-cultured cells in a moderate manner (Fig. 1A). We further examined AMPK phosphorylation by treating cells with 10 mM salicylate for different time periods (5 min, 30 min, 3 h, 6 h, 12 h, 24 h) in the absence or presence of serum. In both culture conditions, we found that salicylate activated AMPK within the first 5 min and this activation maintained for at least 24 h (Fig. 1B). These results suggest that salicylate rapidly induces AMPK activation in metastatic breast cancer cells.

Salicylate inhibits hyaluronan biosynthesis and accumulation in breast cancer cells

AMPK phosphorylates and inactivates HAS2 [27]. We therefore investigated whether salicylate inhibits

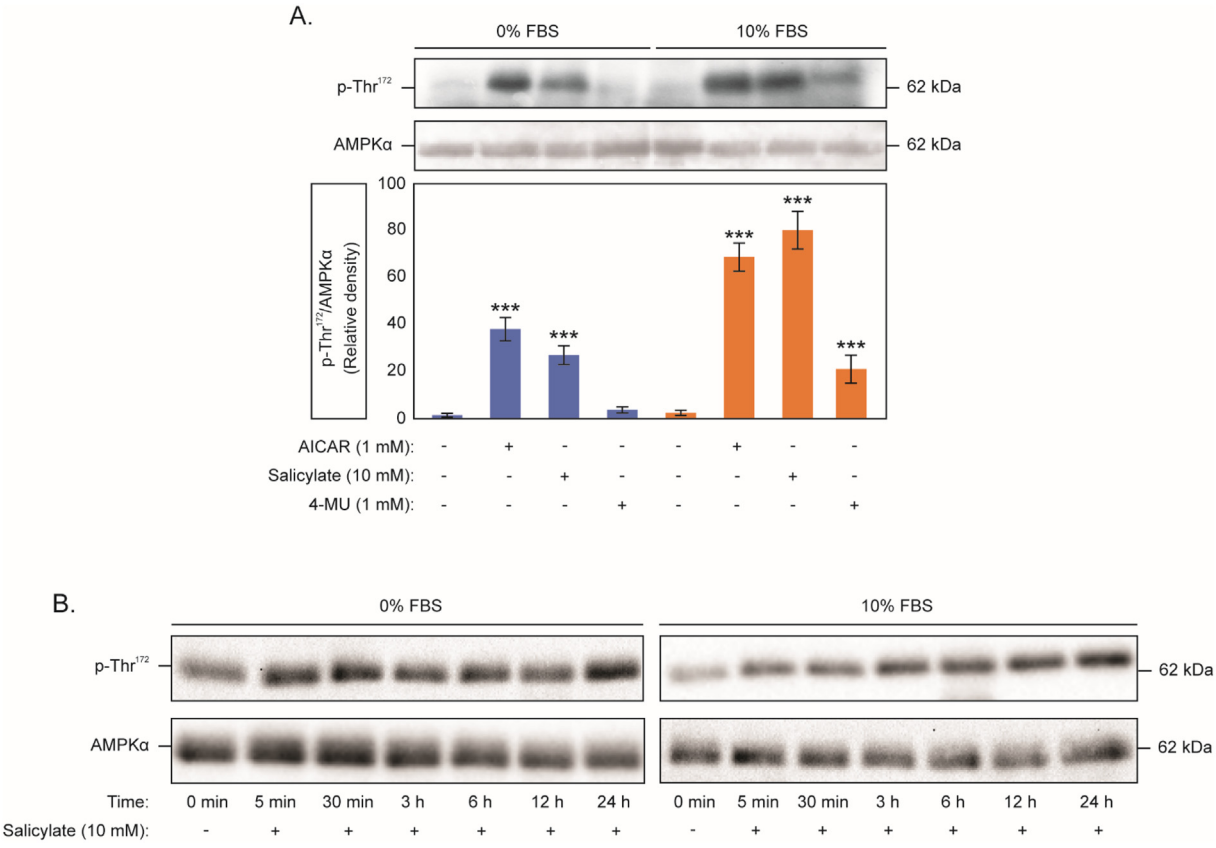

Fig. 1. Salicylate activates AMPK in metastatic breast cancer cells. Immunoblot analyses ($n = 4$) of phosphorylated AMPK at Thr^{172} in the α subunit and total AMPKα after (A) treatment with AICAR (1 mM), salicylate (10 mM) and 4-MU (1 mM) for 24 h, and (B) treatment with salicylate (10 mM) for various time periods (0 min, 5 min, 30 min, 3 h, 6 h, 12 h, 24 h), in the absence (0%) or presence (10%) of serum (FBS). Statistical differences with untreated cells are indicated with black asterisks (***$p < 0.001$).

hyaluronan biosynthesis through activation of AMPK. We first performed immunofluorescence analysis for cell-associated (i.e. intracellular and membrane-bound) hyaluronan. Under baseline conditions, different subcellular distributions of hyaluronan were observed depending on the absence or presence of serum. In the serum-starved cells, intracellular hyaluronan was found condensed in the perinuclear zone while in the presence of serum it appeared more diffuse in the cytosol (Fig. 2A). Regarding the membrane-bound hyaluronan, it was present throughout the cell in the absence of serum but showed a patchy pattern when cells were cultured with serum (Fig. 2A). Notably, salicylate caused a significant re-distribution and reduction of cell-associated (intracellular and membrane-bound) hyaluronan in serum-starved cells which was, however, less obvious in cells cultured in 10% FBS (Fig. 2A). These changes were associated with significant cellular morphological alterations since salicylate-treated cells appeared more elongated (Fig. 2A).

To further explore the effect of salicylate on hyaluronan production, we quantified total hyaluronan secreted by MDA-MB-231 cells following a 6 h, 12 h and 24 h incubation with increasing concentrations (5, 10 and 20 mM) of salicylate in the absence or presence of serum. The results showed that serum-starved cells synthesized lower hyaluronan amounts compared to those cultured with serum (Fig. 2B). Interestingly, salicylate caused a dose-dependent decrease of hyaluronan production at all time points, which was more obvious when cells were cultured in the presence of serum (Fig. 2B). To evaluate the effect of salicylate on non-malignant cells, we quantified hyaluronan secreted by normal skin fibroblasts treated with salicylate in the absence or presence of serum. The results revealed that salicylate caused a significant dose-dependent decrease of hyaluronan production under both culture conditions also in these cells (Supplementary Fig. 1A).

Overall, these results suggest that salicylate suppresses hyaluronan synthesis, secretion and

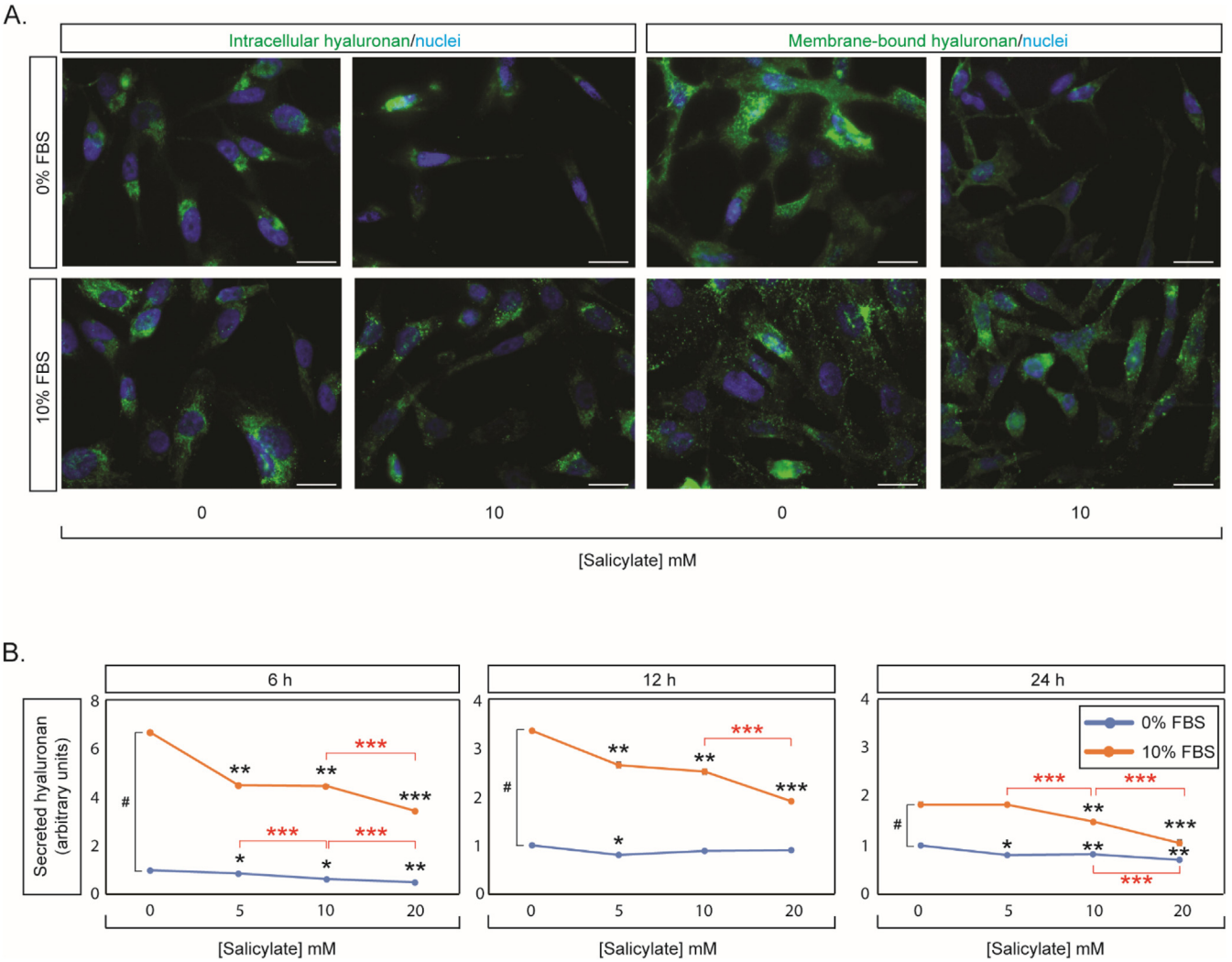

Fig. 2. Salicylate inhibits hyaluronan biosynthesis and secretion in metastatic breast cancer cells. (A) Immunofluorescence analysis of intracellular and membrane-bound hyaluronan was performed with biotin-HABP (green) in MDA-MB-231 cells treated for 24 h with PBS (0 mM, control) or salicylate (10 mM) in the absence (0%) or presence (10%) of serum (FBS). Nuclei are shown in blue (DAPI). Scale bars ~40 μm. (B) Quantification of secreted hyaluronan amounts by a microtiter-based assay in conditioned media of MDA-MB-231 breast cancer cells treated for 6, 12 and 24 h with salicylate (5, 10 and 20 mM) in the absence (0%) or presence (10%) of serum (FBS). The values represent the mean ± SD of 3 independent experiments run in triplicate. Statistical differences (*$p < 0.05$, **$p < 0.01$, ***$p < 0.001$) between salicylate-treated and control (0 mM) cells, and between different treatments are indicated with black and red asterisks, respectively. Statistical differences between serum-starved cells (0% FBS) and cells cultured in the presence of serum (10% FBS) are indicated with hashtag ($^{\#}p < 0.001$).

accumulation in metastatic breast cancer cells as well as in non-malignant cells.

Salicylate affects hyaluronan metabolizing enzymes (HASs, HYALs) and CD44 receptors in breast cancer cells

The significant decrease in cell-associated and secreted hyaluronan, led us to examine whether salicylate also affects the expression of hyaluronan metabolizing enzymes, i.e. hyaluronan synthases (HAS1, HAS2 and HAS3) and the two key hyaluronan-degrading enzymes (HYAL-1 and HYAL-2), as well as various isoforms of the main hyaluronan receptor CD44 (CD44s, CD44v3, CD44v6, and CD44v9). As shown in Fig. 3A, salicylate significantly repressed (about 50%, $p<0.001$) *HAS2*, the main hyaluronan synthase in MDA-MB-231 cells, and to a lesser extent *HAS1* ($p<0.05$). In contrast, salicylate induced *HAS3* ($p<0.05$). The observed substantial inhibitory effect of salicylate on *HAS2* mRNA levels, prompted us to monitor the expression of *HAS2* in MDA-MB-231 cells following a 6 h, 12 h and 24 h incubation with salicylate, in the absence or presence of serum. The results confirmed the significant down-regulation of *HAS2* in serum-starved cells after 24 h treatment with salicylate, which was also evident at earlier time point (12*h*) ($p<0.01$, Fig. 3B). However, when cells were cultured in serum, salicylate did not exhibit any appreciable effect on *HAS2* expression (Fig. 3B).

Regarding hyaluronan-degrading enzymes, salicylate was found to induce *HYAL-2* ($p<0.05$, Fig. 3A), which is the main hyaluronidase in MDA-MB-231 cells, while it reduced *HYAL-1* about 40% ($p<0.01$, Fig. 3A). However, exposure of the cells to salicylate did not result in the production of fragmented hyaluronan in the conditioned medium indicating no apparent induction of hyaluronidase activity (Supplementary Fig. 3). Furthermore, treatment with salicylate caused a strong induction (about 70%) of the main CD44 form *(CD44s)* in these cells ($p<0.001$, Fig. 3A), while it also significantly upregulated the expression of specific CD44 isoforms (*CD44v3* and *CD44v9*) (Fig. 3A).

Collectively, our results indicate that salicylate globally affects hyaluronan-related molecules (i.e. HASs, HYALs, CD44) at the transcriptional level in these cells.

Salicylate suppresses breast cancer cell viability and proliferation

In order to investigate whether the effect of salicylate on hyaluronan affects breast cancer cell functional properties, we exposed cells to increasing concentrations of the drug for different time periods and recorded the effects on cell viability and proliferation. In a short-term (48 h) experiment, MDA-MB-231 cells were treated with 5, 10 or 20 mM salicylate in the absence or presence of serum. Under both culture conditions, we found a significant reduction in cell proliferation and viability, which was more pronounced in cells cultured in the presence of serum (Fig. 4A). Serum-starved cells reacted at 5 mM of salicylate (approx. 40% reduction, $p<0.001$) and remained at similar levels also with higher concentrations (10 and 20 mM) of the drug (Fig. 4A). On the other hand, when cells were cultured in the presence of serum, this reduction was dose-dependent reaching about 80% at the highest concentration of salicylate (20 mM, $p<0.001$, Fig. 4A). Similar results on cell viability with regard to drug concentration and culture conditions were obtained for the metastatic Hs 578T breast cancer cell line (Supplementary Fig. 2A). To further examine the effect of salicylate on cell viability, we performed a long-term experiment (up to 10 days) with MDA-MB-231 cells exposed to increasing concentrations of salicylate in the presence of serum. The results revealed a significant reduction in cell viability and proliferation that reached over 90% at all concentrations used (5, 10 and 20 mM) on day 10 compared to untreated cells ($p<0.001$, Fig. 4B). However, salicylate did not affect the viability and proliferation of non-malignant cells (normal skin fibroblasts) at all concentrations used (5, 10 and 20 mM) in this study (Supplementary Fig. 1B).

To further investigate these observations, we performed immunoblotting analyses for cyclin D1 and cleaved caspase-3, which play central roles in the regulation of cell cycle progression and induction of apoptosis, respectively. Notably, the results revealed a substantial decrease of cyclin D1 protein levels with increasing concentrations of salicylate (Fig. 4C). On the other hand, salicylate treatment did not result in any effect on caspase-3 (Fig. 4C). Altogether, these data suggest that salicylate potently suppresses the growth of metastatic breast cancer cells by promoting cell cycle arrest rather than by inducing apoptosis.

Salicylate attenuates breast cancer cell migration

Next, we performed wound-healing assays with increasing concentrations of salicylate for different time periods (6, 12, 24, 48 h) in the absence or presence of serum in order to evaluate the effect of the drug on breast cancer cell migration. In the presence of serum, we found a significant inhibition in the migratory potential of MDA-MB-231 cells at all concentrations of salicylate 24 h and 48 h post-treatment, with the effect becoming evident within 12 h with the highest concentration (20 mM) of the drug (Fig. 5A). The reduction was less pronounced in serum-starved cells which, however, already reacted within 6 h at the higher concentrations (10 and

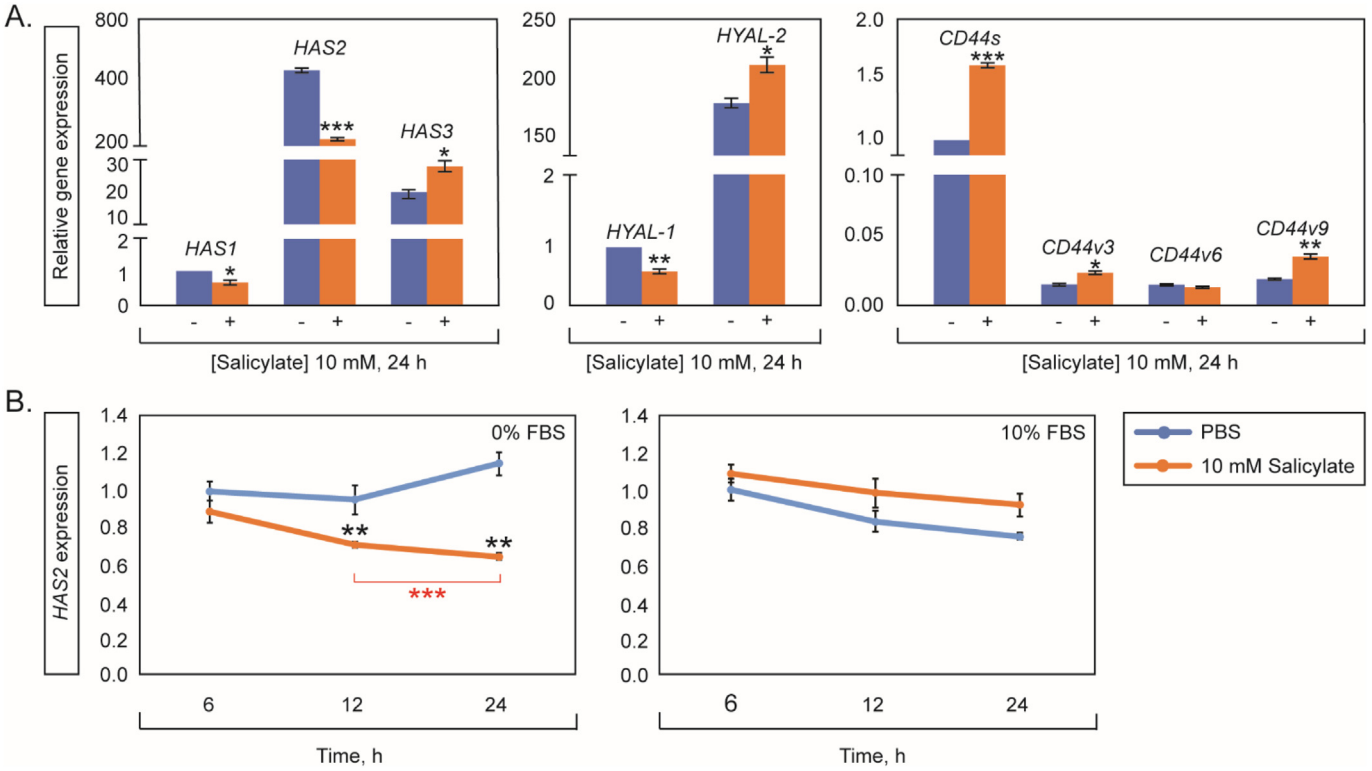

Fig. 3. Salicylate affects the expression of hyaluronan metabolizing enzymes (HASs, HYALs) and CD44 receptors in metastatic breast cancer cells. (A) Quantitative qPCR analyses of *HAS1*, *HAS2*, *HAS3*, *HYAL-1*, *HYAL-2*, *CD44s*, *CD44v3*, *CD44v6* and *CD44v9* after treatment with 10 mM salicylate for 24 h in the absence (0%) of serum (FBS). (B) Quantitative qPCR analysis of *HAS2* expression after treatment with 10 mM salicylate for 6, 12 and 24 h in the absence (0%) or presence (10%) of serum (FBS). The values represent the mean ± SD of 3 independent experiments run in triplicate. Statistical differences (*$p < 0.05$, **$p < 0.01$, ***$p < 0.001$) between salicylate-treated and control (0 mM) cells, and between different treatments are indicated with black and red asterisks, respectively.

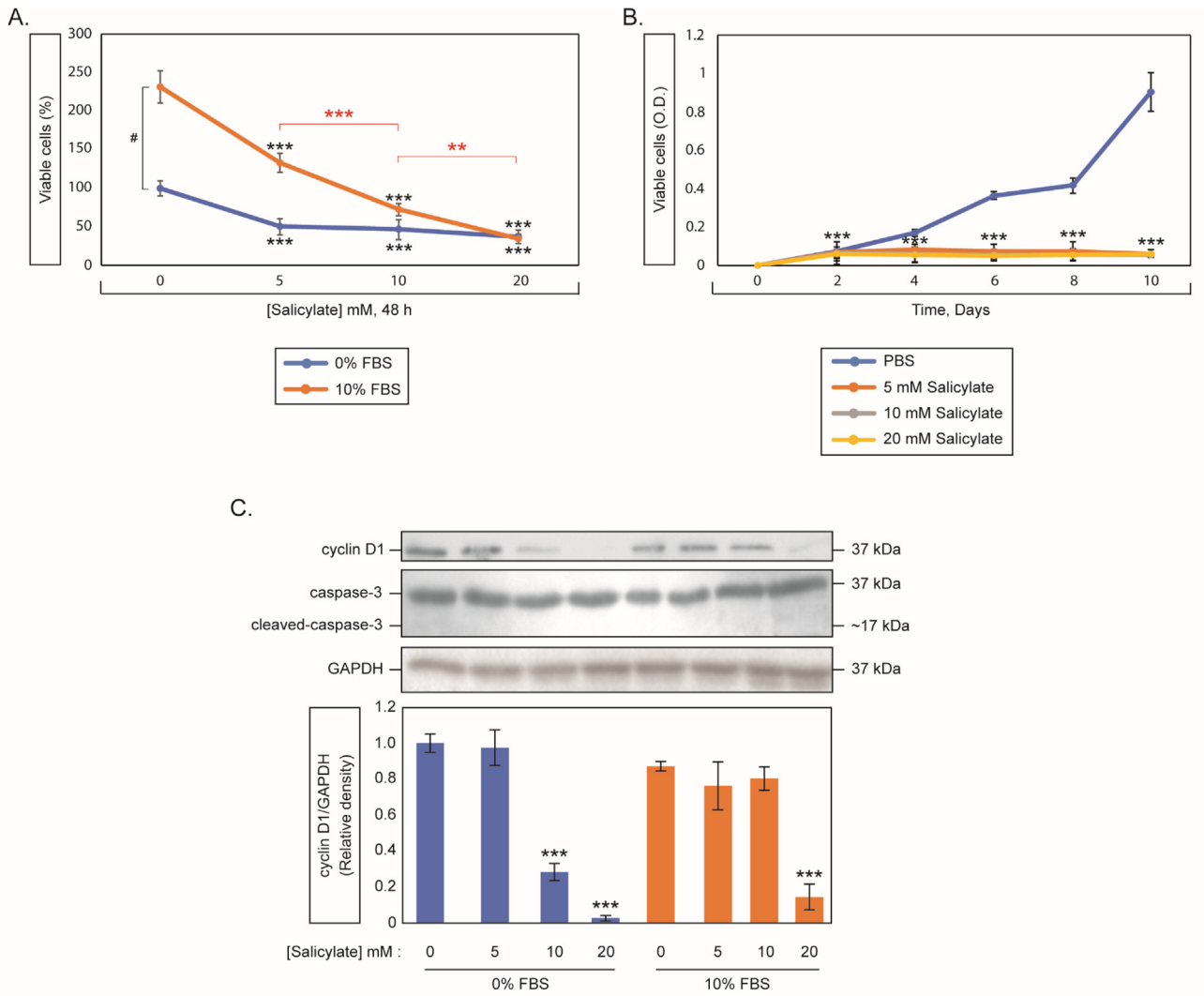

Fig. 4. Salicylate suppresses metastatic breast cancer cell viability and growth. Cell viability after treatment with PBS (0 mM, control) or increasing concentrations of salicylate (5, 10 and 20 mM) in the absence (0%) or presence (10%) of serum (FBS) for (A) 48 h (short exposure) and (B) 2, 4, 6, 8 and 10 days (long exposure). The values represent the mean ± SD of 3 independent experiments run in triplicate. (C) Immunoblot analyses (n = 3) of cyclin D1, total and cleaved caspase-3, and GAPDH in control or salicylate-treated MDA-MB-231 cells in the absence (0%) or presence (10%) of serum (24 h post-treatment). Statistical differences (**$p < 0.01$, ***$p < 0.001$) between salicylate-treated and control (0 mM) cells, and between different treatments are indicated with black and red asterisks, respectively. Statistical differences between serum-starved cells (0% FBS) and cells cultured in the presence of serum (10% FBS) are indicated with hashtag ($^{\#}p < 0.001$).

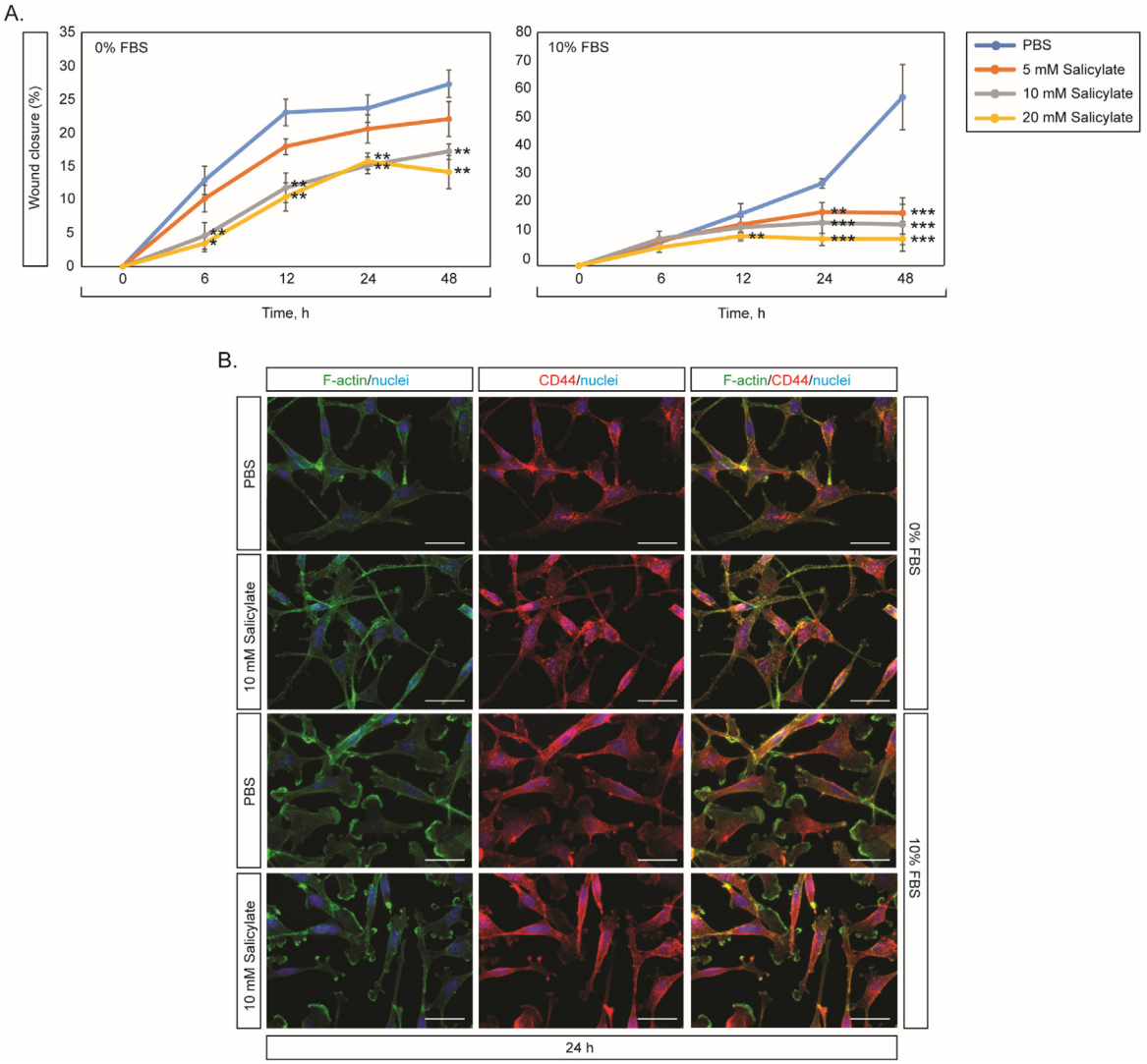

Fig. 5. Salicylate induces changes in actin cytoskeleton and CD44 distribution, and inhibits the migration of metastatic breast cancer cells. (A) Migration of MDA-MB-231 cells treated with PBS (0 mM, control) or increasing concentrations of salicylate (5, 10 and 20 mM) in the absence (0%) or presence (10%) of serum (FBS). The values represent the mean ± SD of 4 independent experiments run in triplicate. Statistical differences between salicylate-treated and control cells are indicated with black asterisks (*$p < 0.05$, **$p < 0.01$, ***$p < 0.001$). (B) Immunofluorescence analysis for filamentous actin (F-actin, green) and CD44 (red) in MDA-MB-231 cells exposed to PBS or 10 mM salicylate for 24 h in the absence (0%) or presence (10%) of serum (FBS). Nuclei are shown in blue (DAPI). Scale bars ~40 µm.

20 mM) of salicylate (Fig. 5A). The suppressive effect of salicylate on metastatic breast cancer cell migration was further supported by the potent inhibition of Hs 578T cell motility after treatment with increasing concentrations of the drug (Supplementary Fig. 2B).

Since the migratory potential of the cells is closely associated with their cytoskeletal changes, we performed immunofluorescence analysis using Phalloidin-iFluor^{488} to visualize actin filaments (F-actin). Cells cultured in the presence of serum exhibited a well-organized actin cytoskeleton showing a more intense staining at cell membrane protrusions compared to serum-starved cells (Fig. 5B). Salicylate induced severe morphological changes to the cells as they became shrinked and elongated followed by perturbation of the actin cytoskeleton (Fig. 5B). Notably, in serum-cultured cells, the drug reduced filamentous actin staining at cell membrane protrusions showing a patchy expression pattern (Fig. 5B).

Next, we used anti-CD44 antibody to visualize the subcellular distribution of the hyaluronan receptor CD44, which often contributes to the cell migratory/invasive potential. While under both culture conditions (0% and 10% FBS) CD44 appeared diffuse in the cytosol and clustered to actin-rich membrane protrusions of the tumor cells, serum-starved cells showed a more patchy expression of the receptor (Fig. 5B). Of note, CD44 signal remained strong (or even stronger in some cases) in salicylate-treated cells, but it was markedly redistributed following the cell shape changes induced by the drug (Fig. 5B). Collectively, salicylate markedly induced changes in actin cytoskeleton organization and overall breast cancer cell morphology with a concurrent redistribution of hyaluronan receptor CD44.

Salicylate enhances breast cancer cell adhesiveness

The observed inhibitory effect of salicylate on breast cancer cell motility prompted us to investigate the adhesive capacity of salicylate-treated MDA-MB-231 cells to collagen type I matrices in the absence or presence of serum. To this end, we exposed cells to increasing concentrations (5, 10, and 20 mM) of salicylate for 24 h, which were then transferred to dishes pre-coated with collagen type I and incubated for 30 min. Counting of adherent cells revealed that salicylate significantly induced cell adhesion in the presence of serum (Fig. 6A). However, serum deprivation resulted in lower tumor cell adhesion, which was moderately enhanced after treatment with 10 mM salicylate (Fig. 6A).

To further investigate these observations, we performed immunofluorescence analyses of the cells grown on collagen type I matrices. In the presence of serum, cells appeared more rounded with intense presence of actin filaments at the cell periphery, which was not the case for serum-starved cells (Fig. 6B). Salicylate induced cell rounding also under serum-free conditions, while it evoked actin cytoskeleton reorganization under both culture conditions (Fig. 6B). Notably, salicylate appeared to promote actin-rich cell-cell contacts in serum-starved cells, which were less obvious in cells cultured under nutrient-rich conditions (arrows, Fig. 6B). This observation is reinforced by the finding of the induction of E-cadherin expression solely in serum-starved cells after salicylate treatment (Fig. 6C). Furthermore, immunofluorescence analysis of cells grown on collagen type I for CD44 showed a remarkable redistribution of the receptor after salicylate treatment, which was localized primarily in the perinuclear zone (mainly in cells cultured in the presence of serum) (Fig. 6B). Collectively, these results suggest that salicylate promotes breast cancer cell adhesiveness via different mechanisms depending on nutrient availability in the microenvironment of the cell.

Discussion

Hyaluronan promotes tumorigenesis, cancer metastasis, and chemoresistance. Cell-associated (pericellular, intracellular) hyaluronan influences virtually all cell-cell and cell-matrix interactions, controlling cell growth, apoptosis, motility, differentiation, epithelial to mesenchymal transition, and stem cell functions [4,6,8,15,17,43]. In breast cancer, HAS enzyme levels are related to poor differentiation, tumor aggressiveness and poor prognosis for patients [2–4,44]. It has been proposed that the high expression of HAS2 and CD44 in ER-negative breast cancer cells might have a significant clinical relevance in controlling TNBC distant metastasis [2]. Notably, silencing or antisense inhibition of HAS2 suppressed the malignant phenotype of invasive breast cancer cells and inhibited the formation of tumors in vivo [45,46]. In line with this, we recently reported that 4-MU exhibited tumor-suppressive functions in mammary carcinoma cells of distinct malignant phenotypes and estrogen receptor status suggesting that hyaluronan synthesis inhibition could represent an emerging therapeutic approach with significant clinical relevance in controlling different breast cancer subtypes [47].

The finding that salicylate, which is rapidly formed in vivo after aspirin (acetyl salicylate) administration, can directly activate AMPK [42], a kinase that is known to phosphorylate and inactivate HAS2 [27], led us to investigate whether salicylate inhibits hyaluronan biosynthesis.

The therapeutic effects of aspirin and salicylate in inflammation and cancer were thought to be exerted through multiple mechanisms, predominately via

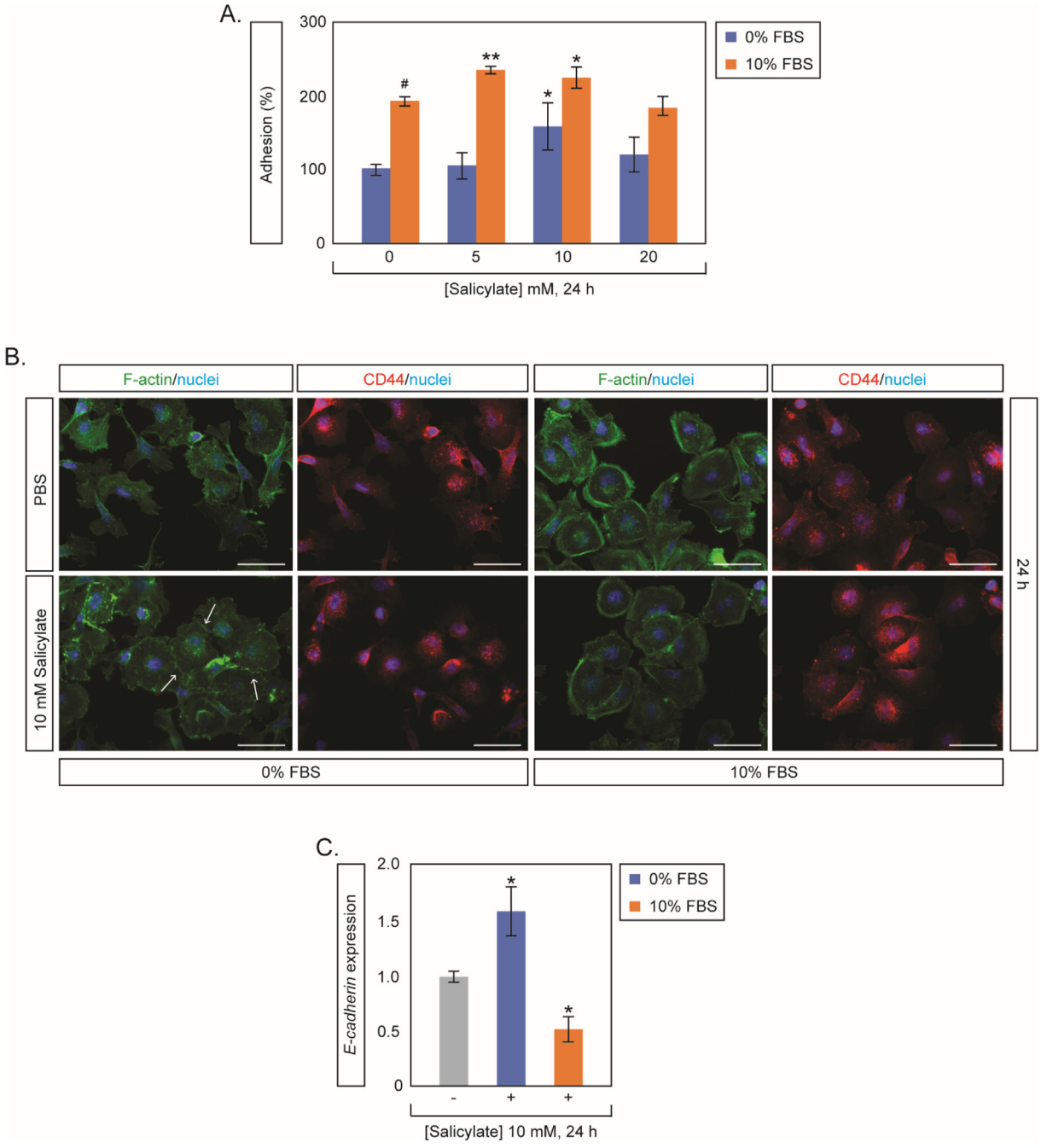

Fig. 6. Salicylate enhances the adhesiveness of metastatic breast cancer cells. (A) Adhesion of MDA-MB-231 cells on collagen type I matrix after treatment with PBS (0 mM, control) or increasing concentrations of salicylate (5, 10 and 20 mM) for 24 h in the absence (0%) or presence (10%) of serum. (B) Immunofluorescence analysis of cells treated for 24 h with PBS or 10 mM salicylate for filamentous actin (F-actin, green) and CD44 (red) in the absence (0%) or presence (10%) of serum. Nuclei are shown in blue (DAPI). Arrows point at newly formed cell-cell contacts. Scale bars ~40 μm. (C) Quantitative qPCR analysis of *E-cadherin* expression after salicylate (10 mM) treatment for 24 h in the absence (0%) or presence (10%) of serum. The values represent the mean ± SD of 3 independent experiments run in triplicate. Statistical differences between salicylate-treated and control (0 mM) cells are indicated with black asterisks (*$p \leq 0.05$, **$p \leq 0.01$). Statistical differences between serum-starved cells (0% FBS) and cells cultured in the presence of serum (10% FBS) are indicated with hashtag ($^{\#}p < 0.001$).

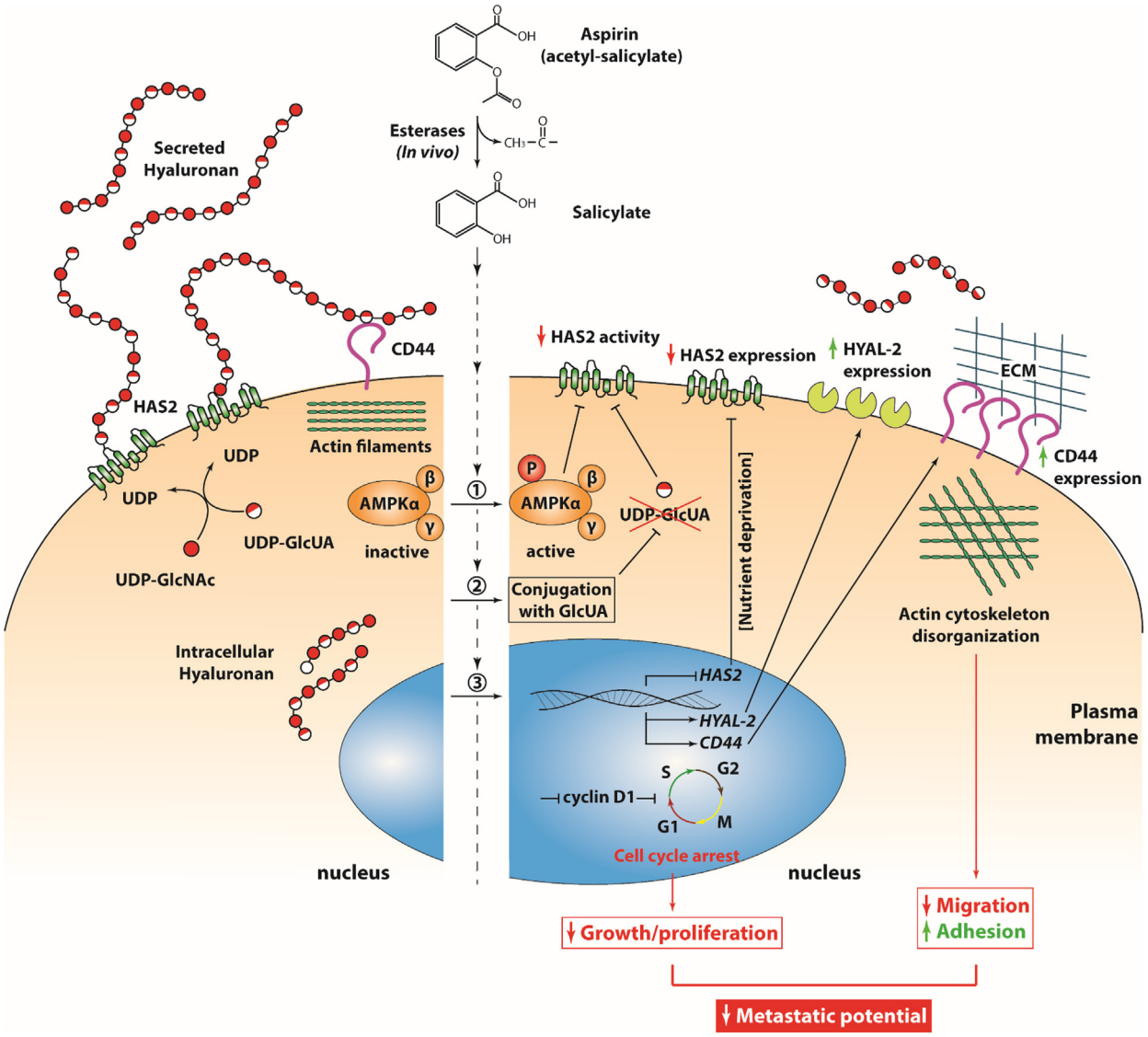

Fig. 7. Proposed model of salicylate-mediated onco-suppressive effects in metastatic breast cancer cells. Salicylate inhibits hyaluronan biosynthesis and accumulation through: (1) phosphorylation and activation of AMPK, (2) conjugation with precursor substrates (UDP-GlcUA), (3) down-regulation of *HAS2* (in nutrient deprivation conditions) and up-regulation of *HYAL-2*. These changes are followed by the repression of cyclin D1 and the marked redistribution of actin filaments and CD44 resulting in inhibition of cell proliferation/growth and cell motility, respectively. For details, see text.

COX inhibition and NF-κB pathway modulation [48,49]. However, additional mechanisms have been also proposed, including direct allosteric activation of AMPK [42,50], mTOR signaling inhibition and induction of autophagy [50], regulation of epigenetic effectors like CBP/p300 [38] as well as tumor microenvironment modulation as evidenced by the inhibition of the tumor-promoting and angiogenic matrix-degrading enzymes heparanase [40] and uPA [41]. These studies suggest that salicylate and aspirin influence several molecular pathways and that their anti-cancer activities can be attributed to multiple targets.

Our study adds to the target spectrum of these drugs, since we show for the first time that salicylate affects the hyaluronan molecular network. This effect was accompanied by a significant repression of the malignant phenotype of metastatic breast cancer cells. The observed onco-suppressive properties of salicylate on breast cancer cells are in line with the effects of aspirin and salicylate on various types of malignant tumors [38,40,51–54]. The results of the present study support a model where salicylate rapidly activates AMPK and causes a dose-dependent reduction of cell-associated (i.e. intracellular and membrane-bound) hyaluronan as well as in the extracellular space. The inhibitory effect of salicylate on hyaluronan production in metastatic breast cancer cells seems to have occurred at several levels (see Fig. 7). First, salicylate activated AMPK, as evidenced by the increased phosphorylation of Thr^{172} on AMPK-α (Fig. 1), promoting phosphorylation of HAS2 [27], the main HAS in MDA-MB-231 cells [47], thereby inhibiting hyaluronan biosynthesis. Second, salicylate modulated the major hyaluronan metabolizing enzymes (i.e. HAS2 and HYAL-2) in this breast cancer cell model at the transcriptional level with no, however, apparent changes in hyaluronidase activity. The observation of a more obvious decrease of secreted hyaluronan in cells cultured with serum compared to serum-starved cells already at 6 h after treatment with salicylate (Fig. 2B) without remarkable alterations in HAS2 mRNA levels (Fig. 3B) supports the hypothesis that salicylate affected the hyaluronan synthesizing capacity of these cells mainly through AMPK activation that reached its highest levels in the same time frame (Fig. 1B). We would like to note out that the observation that serum-starved cells synthesized low hyaluronan amounts could be due to autophagic clearance of HAS2 evoked by the nutrient deprivation, which is a novel mechanism for hyaluronan suppression recently demonstrated by Chen and colleagues [55]. As a consequence, the effect of salicylate on secreted hyaluronan from these cells is moderate. Third, according to the literature, salicylate could conjugate with glucuronic acid to form salicyl phenolic glucuronide and salicyl acyl glucuronide during its metabolic processing [33,56]. This raises the possibility that salicylate may interfered with the generation of the UDP-precursors (i.e. UDP-GlcUA) needed for hyaluronan synthesis. As a result, UDP-GlcUA availability was reduced, UDP-GlcUA concentration declined in the cytosol and hyaluronan synthesis was inhibited. However, this possibility remains to be elucidated in this breast cancer cell model.

Our findings further suggest that salicylate inhibits breast cancer cell proliferation and growth by inducing cell cycle arrest rather than apoptosis. This is in line with previous observations where salicylate induced cell cycle changes in MDA-MB-231 cells [41] and acetyl salicylate inhibited the proliferation of vascular smooth muscle cells and colon adenocarcinoma cells by halting cell cycle progression without inducing apoptosis [57,58]. Interestingly, in ER-positive breast cancer cells, combined treatment with aspirin and tamoxifen (an ER antagonist) down-regulated *cyclin D1* and blocked cell cycle in G0/G1 phase [59]. However, other studies have reported an apoptotic response of tumor cells to aspirin suggesting cell-type and context-specific mechanisms [60]. Furthermore, the altered subcellular topology of hyaluronan and CD44 after salicylate treatment suggests their possible involvement in cyclin D1 down-regulation, since it has been shown that the translocation of CD44 to the nucleus induces STAT3/p300 complex formation and binding to the *cyclin D1* promoter to induce its expression and cell proliferation [61]. Finally, the possibility that salicylate-mediated suppression of proliferation could be also due to the substantial decrease of cell-associated hyaluronan should not be excluded given the established promoting roles of intracellular and membrane-bound hyaluronan in mitosis and cell proliferation [8,62]. Importantly, the inappreciable effect of salicylate on non-malignant cell growth and proliferation further supports its use in vivo as a potential anti-cancer modality with no or minimal side effects.

The inhibitory effect of salicylate on the motility of metastatic breast cancer cells observed within the first 24 h of treatment could be associated with the marked decrease of membrane-bound (Fig. 2A) and secreted hyaluronan (Fig. 2B) as well as the significant cell morphological changes induced by the drug in the same time frame (Fig. 5B). Due to their hydroscopic properties, hyaluronan molecules are known to create favorable microenvironments for the cells to proliferate and migrate [63]. Therefore, their elimination from the pericellular area could decrease mammary tumor cells' migratory potential. Moreover, the salicylate-mediated subcellular redistribution of CD44, which showed a diffused pattern followed by its reduced presence in cell protrusions, together with the marked disorganization of actin microfilaments, are compatible with a less motile phenotype. This concept is also supported by the

salicylate-evoked inhibition of the activity of certain components of the plasminogen activation system in MDA-MB-231 cells, such as uPA [41], which are known to create a localized microenvironment of elevated matrix degradation by activating multiple proteolytic pathways facilitating migration and invasion of cancer cells [64]. The reduced migration of breast cancer cells after salicylate treatment is further illustrated by their increased adhesive capacity on collagen type I matrices (Fig. 6A) and the appearance of newly formed cell-cell contacts (Fig. 6B, arrows) followed by E-cadherin up-regulation (Fig. 6C) all of which are associated with a less motile phenotype. Importantly, the underlying mechanisms responsible for the adhesiveness of metastatic breast cancer cells seem to differentiate depending on microenvironmental nutrient availability. It should be noted that the inclusion of the cytostatic agent cytarabine in all wound-healing assays supports the conclusion that the scratch repopulation was not influenced by cell proliferation.

The fact that cyclooxygenases are major targets of salicylate and its acetylated derivative, aspirin, together with the observation that COX-2 is markedly elevated in cancer cells [65,66] have led to the assumption that the onco-suppressive potential of the drugs might be also due to inhibition of COX-2. However, this is yet unclear and most of the studies suggest COX-independent anticancer mechanisms since they have demonstrated that aspirin suppresses proliferation and growth of several cancer cell types regardless of COX-2 expression levels [51–54,67]. Our finding that salicylate inhibits hyaluronan biosynthesis could suggest an additional anticancer mechanism that could involve COX-2, since it has been shown that hyaluronan-CD44 interactions promote activation of COX-2 signaling and cancer cell survival [68]. However, this possibility remains to be elucidated in this breast cancer cell model.

Although both aspirin and salicylate have been widely used anti-inflammatory drugs for years, recent epidemiological and preclinical studies as well as clinical trials have revealed the therapeutic potential of aspirin in patients with cancer of various types (reviewed in [33]). For instance, a retrospective analysis of TNBC patients showed that aspirin increased disease-free survival rate and reduced the risk of metastasis [69].

In conclusion, we discovered that hyaluronan, a pro-angiogenic, pro-inflammatory and tumor-promoting glycosaminoglycan, is a target of salicylate. Our findings provide new mechanistic insights that could explain, at least in part, the anticancer effects of aspirin through modulation of specific constituents of the tumor cell microenvironment. One caveat is the high-dose of aspirin required to activate AMPK in vivo and inhibit endogenous hyaluronan biosynthesis and accumulation in tumor cells. Of note, peak plasma concentrations and half-life of salicylate are orders of magnitude higher than those of acetyl salicylate [34]. The present study offers a direction for the development of new matrix-based therapeutic schemes, utilizing existing low-cost drugs with beneficial effects in yet incurable specific breast cancer subtypes. The status of mutations in oncogenes as well as the expression levels or activity of aspirin/salicylate targets such as COX, CDK, uPA, heparanase, hyaluronan/HAS2 may help identify cancer patients who may benefit from these drugs. Undoubtedly, further studies and randomized clinical trials are necessary to validate aspirin/salicylate-included regimens.

Materials and methods

Cell culture and reagents

The MDA-MB-231 and Hs 578T (highly metastatic; triple negative, ERα-/PR-/HER2-) breast cancer cell lines were obtained from the American Type Culture Collection (ATCC). Human normal skin fibroblasts (AG01523) were kindly provided by Dr. Kletsas (Laboratory of Cell Proliferation & Ageing, National Centre for Scientific Research 'Demokritos', Athens, Greece). Cells were routinely cultured in complete medium [Dulbecco's Modified Eagle's Medium (DMEM, #LM-D1110/500, Biosera) supplemented with 10% fetal bovine serum (FBS, #FB-1000/500, Biosera) and antimicrobial agents cocktail (100 IU/mL penicillin, 100 μg/mL streptomycin, 10 μg/mL gentamycin sulfate and 2,5 μg/mL amphotericin B)] at 37 °C, 95% humidified air/5% CO_2. Fresh medium was added to the cultures every two days. Upon reaching 80% confluency, cells were detached with trypsin-EDTA 1× in PBS for 3 min (#LM-T1706/500, Biosera) and seeded in a new petri dish. Depending on the experiment, the assays were conducted in the absence (serum-deprived) or presence of 10% FBS. Sodium salicylate (#106601) was obtained from Merck Millipore. All chemicals used in the present study were of the best commercially available grade.

Secreted hyaluronan quantification with solid phase assay

The determination of secreted hyaluronan by breast cancer cells was performed as described previously [25]. Shortly, $4\text{-}5 \times 10^4$ MDA-MB-231 cells per well were seeded in a 24-well plate in complete medium for 24 h. The medium was then replaced with serum free medium and the cells were starved overnight (16–18 h). The next day, the cells were incubated with 0, 5, 10 and 20 mM salicylate diluted in DMEM with 0% or 10% FBS for 6, 12 and 24 h. Conditioned media were then collected and

stored at –20 °C until further analysis. Cells were stained with crystal violet (see below) for cell number normalization in hyaluronan concentration determination. Nunc MaxiSorp® flat-bottom 96-well microtiter plates (#44-2404, Invitrogen, Thermo Scientific) were pre-coated overnight with 100 µL per well of 1 µg/mL HABP (Hyaluronan binding protein) diluted in 50 mM carbonate buffer (pH 9,5) at 4 °C. Subsequently, the wells were blocked with 1% BSA/PBS for 1 h at room temperature at 300 oscillations on a bench rocker. Following their dilution (1:8 in 1% BSA/PBS), conditioned media (100 µL) were added to each well (in triplicates) and were incubated for 1 h at room temperature. Next, 100 µL of bHABP (biotinylated-HABP) 0.5 µg/mL in 1% BSA/PBS were added to each well and incubated for 1 h at room temperature followed by incubation with 100 µL of peroxidase-conjugated streptavidin (1:1,600 diluted, #SA202, EMD Millipore) for 1 h at room temperature and, then, incubation with 100 µL of 3,3′,5,5′-tetramethyl-benzidine (#34028, Thermo Scientific) for 3–4 min at room temperature. Finally, 50 µL 2 M H_2SO_4 per well were added to stop the reaction and the absorbance was measured at 450 nm using a TECAN photometer, utilizing Magellan 6.

Short-term cell proliferation assay

The assay was carried out as described by Feoktistova and colleagues [70]. Shortly, 5×10^4 (for 0% FBS) and 4×10^4 (for 10% FBS) MDA-MB-231 cells were seeded in each well of 24-well plate and incubated for 24 h. Following an overnight (16–18 h) incubation with serum free medium, cells were incubated with 0, 5, 10 and 20 mM salicylate diluted in DMEM with 0% or 10% FBS for 48 h. Then, the cells were washed twice with PBS and stained with 200 µL per well 0.5% (*w*/*v*) crystal violet solution in 20% methanol/distilled water for 20 min at room temperature with 150 oscillations on a bench rocker. Staining solution was removed and the excess dye was washed away using tap water, followed by two washes with distilled water. The stained cells were left to dry at room temperature overnight. Then, methanol (200 µL) was added to each well and the cell-bound dye was retrieved after 20 min incubation of the plate at 150 oscillations on a bench rocker at room temperature. Optical density of each well was measured at 570 nm using a TECAN photometer, utilizing Magellan 6.

Long-term cell proliferation assay

5×10^3 MDA-MB-231 cells were seeded in each well of 24-well plate and incubated with complete medium for 24 h. The cells were then incubated with 0, 5, 10 and 20 mM salicylate diluted in DMEM with 10% FBS. Every two days, fresh medium containing salicylate in the appropriate concentrations was added to the cells. At desired time periods (2, 4, 6, 8 and 10 days), the cells were stained with crystal violet solution and methanol (200 µL) was added to each well to retrieve the cell-bound dye after 20 min incubation. Optical density of each well was measured at 570 nm as described above.

Wound healing assay

The assay was performed as described previously [47]. In brief, 25×10^4 (for 0% FBS) and 20×10^4 (for 10% FBS) MDA-MB-231 cells were seeded in each well of a 12-well plate in complete medium. After 24 h incubation, cells were serum starved overnight (16–18 h). Cell monolayers were scratched using a pipette tip and washed twice with Dulbecco's Phosphate Buffered Saline (PBS, #LM-52041/500, Biosera). The cells were then incubated with DMEM containing 0, 5, 10, 20 mM salicylate with or without 10% FBS and 10 µM cytarabine (Pfizer) for the desired time periods. Photos were captured at 0, 6, 12, 24 and 48 h utilizing a color digital camera (CMOS) mounted on a phase contrast microscope (OLYMPUS CKX41, QImaging Micro Publisher 3.3RTV) through a 10× objective. The images were quantified with Image J 1.50b Launcher Symmetry Software.

Collagen type I cell adhesion assay and immunofluorescence staining

The assay was performed as described previously [47]. Shortly, 30×10^4 (for 0% FBS) and 20×10^4 (for 10% FBS) MDA-MB-231 cells were seeded in 6-well plates in complete medium and incubated for 24 h followed by overnight starvation (16–18 h) with serum free medium. The cells were incubated with 0, 5, 10 and 20 mM salicylate diluted in DMEM with 0% or 10% FBS for 24 h. Afterwards, the cells were dissociated using 5 mM EDTA in PBS (10 min in room temperature), collected, centrifuged, reconstituted in serum free medium containing 0.1% BSA and counted. 25×10^3 cells were seeded and incubated for 30 min to adhere in a pre-coated (with 40 µg/mL collagen type I in PBS at 4 °C overnight) 96-well plate blocked with 1% BSA in PBS for 30 min. Then, cells that didn't adhere were removed with two washes with PBS and each well was stained with 0.5% (*w*/*v*) crystal violet in 20% methanol/distilled water for 20 min at 37 °C at 150 oscillations on a bench rocker. After staining, the procedure was followed as previously described.

For immunofluorescence, the cells were seeded on coverslips pre-coated with 40 µg/mL collagen type I in PBS and the staining was performed as described below.

Immunofluorescence studies

The assay was performed as described before [47]. Briefly, 5×10^4 (for 0% FBS) and 4×10^4 (for 10% FBS) MDA-MB-231 cells were seeded on UV-sterilized glass coverslips and cultured with complete medium for 24 h. The cells were starved overnight (16–18 h) with serum free medium. Next, the cells were incubated with 0, 5, 10 and 20 mM salicylate diluted in DMEM with 0% or 10% FBS for 24 h. The cells were fixed with 4% paraformaldehyde in PBS (pH 7.2–7.4) and permeabilized with 0.05% Triton X-100/PBS-Tween 0.01% for 1 min, followed by quenching with 200 mM glycine in PBS for 30 min at room temperature and blocking with 5% bovine serum albumin (BSA)/PBS-Tween 0.01% for 1 h at room temperature. Afterwards, primary antibody against CD44 (1 μg/mL, Hermes-3 kindly provided by Dr. S. Jalkanen) and Phalloidin-iFluor™ 488 Conjugate (1:40, #00042, Biotium CF™488A) in 1% BSA/PBS-T were added and samples were incubated at 4 °C overnight. The next day, the appropriate secondary antibody was added in 1% BSA/PBS-Tween 0.01% [1:1000, #20110, goat anti-mouse IgG (H + L), Biotium CF™594] and incubated for 1 h in the dark. Finally, the cells were washed with distilled water, stained and mounted with DAPI. Between each step after fixation cells were washed 3 times with PBS-Tween 0.01%. Slides remained in dark overnight and then visualized using a fluorescent phase contrast microscope (OLYMPUS CKX41, QImaging Micro Publisher 3.3RTV) at 60×.

For cell-associated hyaluronan staining, the same protocol with specific modifications was performed. In particular, for the detection of intracellular hyaluronan, fixed cells were treated with 1 U/mL (in PBS) bovine hyaluronidase PH-20 and then permeabilized with 0.05% Triton X-100/PBS. For the detection of membrane-bound hyaluronan, cells were not subjected to any treatment (neither hyaluronidase nor Triton X-100). All washes were performed with PBS/10% ethanol and cells were blocked with 5% BSA/PBS containing blocking solution (4 drops of streptavidin and 4 drops of biotin) to block the endogenous biotin and avidin (#E-21390, Molecular Probes). Hyaluronan was stained with bHABP (4 μg/mL in 1% BSA/PBS) and detected with streptavidin Alexa Fluor™ 488-conjugate (1:1,000 in 1% BSA/PBS, #S11223, Thermofisher Scientific).

RNA isolation, cDNA synthesis, and Real time-PCR

RNA isolation was carried out using the NucleoSpin® RNA, MACHEREY-NAGEL kit according to the manufacturer's instructions. Isolated RNA was quantified by measuring absorbance at 260 nm. cDNA was synthesized using the PrimeScript™ RT reagent Kit (Perfect Real Time), TAKARA (#RR037A) kit according to the manufacturer's instructions. Real time-PCR analysis was conducted in 20 μL reaction mixture, according to the manufacturer's instructions. The amplification was performed utilizing Rotor Gene Q (Qiagen, USA). All reactions were performed in triplicate and a standard curve was always included for each pair of primers for assay validation. In addition, a melting curve analysis was always performed for detecting the SYBR Greenbased objective amplicon. To provide quantification, the point of product accumulation in the early logarithmic phase of the amplification plot was defined by assigning a fluorescence threshold above the background, defined as the threshold cycle (Ct) number. Relative expression of different gene transcripts was calculated by the ΔΔCt method. The Ct of any gene of interest was normalized to the Ct of the normalizer (GAPDH). Fold changes (arbitrary units) were determined as $2^{-\Delta\Delta Ct}$. Genes of interest and utilized primers are presented in Table I.

Western blot analysis

Cells after treatment with the desired agents and time points were washed twice with PBS and stored in –80 °C until use or lysed immediately using RIPA lysis buffer [50 mM Tris-HCl (pH = 8.0), 150 mM NaCl, 1% NP-40, 0.5% sodium deoxycholate, 2% sodium dodecyl sulfate and 100× HALT protease and phosphatase inhibitor cocktail (#1861281, Thermo Fischer Scientific)] at 4 °C for 30 min. Every 10 min the cell pellet was vortexed for 10 s. Then, the samples were centrifuged at 13,000 rpm for 10 min at 4 °C and the supernatants were collected in new eppendorf tubes. Next, 6× SDS-sample buffer [0.5 M Tris-HCl (pH 6.8), 30% (*w/v*) glycerol, 10% (w/v) SDS, 0.6 M DTT, 0.012% (w/v) bromophenol blue] was added and the lysates were boiled at 100 °C for 5 min. The samples were separated by SDS-PAGE in 10% polyacrylamide gels and transferred to nitrocellulose membranes (0.45 μM pore diameter, #10600002, GE Healthcare Life Sciences). The membranes were blocked in 5% (w/v) BSA or skim non-fat dry milk in TBS (pH 7.4) containing 0.05% Tween-20 (TBS-T) for 1 h at room temperature and were then incubated with primary antibodies against: p-AMPKα (rabbit, 1:500, #2535, Cell Signaling), AMPKα (rabbit, 1:500, #2532, Cell Signaling), cyclin D1 (mouse, 1:200, #sc-8396, SANTA CRUZ Biotechnology), caspase-3 (rabbit, 1:1,000, #9665, Cell Signaling), GAPDH (rabbit, 1:2,000, #2118, Cell Signaling) in 1% BSA/TBS-Tween 0.1% + 0.02% NaN_3 for 16–18 h at 4 °C. After three 5-min washes in TBS-T, membranes were incubated with goat anti-rabbit HRP (1:10,000, Thermo Scientific) or goat anti-mouse HRP (1:10,000, Pierce) in 1% BSA or skim non-fat

Table I. Primer sequences used for qPCR.

Gene	Primer sequence	$T_{annealing}$
CD44s	Sense:ATAATAAAGGAGCAGCACTTCAGGA Anti-sense:ATAATTTGTGTCTTGGTCTCTGGTAGC	60 °C
CD44v3	Sense:ATAATGGCTGGGAGCCAAATGAAGAAA Anti-sense:ATAATCATCATCATCAATGCCTGATCCAGA	60 °C
CD44v6	Sense:ATAATCAGAAGGAACAGTGGTTTGGCA Anti-sense:ATAATGTCTTCTTTGGGTGTTTGGCGA	60 °C
CD44v9	Sense:ATAATGAGCTTCTCTACATCACATGAAGGC Anti-sense: TAATGTCAGAGTAGAAGTTGTTGGATGGTC	60 °C
HAS1	Sense:GGAATAACCTCTTGCAGCAGTTTC Anti-sense: GCCGGTCATCCCCAAAAG	60 °C
HAS2	Sense:TCGCAACACGTAACGCAAT Anti-sense:ACTTCTCTTTTTCCACCCCATTT	60 °C
HAS3	Sense:AACAAGTACGACTCATGGATTTCCT Anti-sense:GCCCGCTCCACGTTGA	60 °C
HYAL-1	Sense:GATTGCAGTGTCTTCGATGTGGTA Anti-sense:GGGAGCTATAGAAAATTGTCATGTCA	60 °C
HYAL-2	Sense:CTAATGAGGGTTTTGTGAACCAGAATAT Anti-sense:GCAGAATCGAAGCGTGGATAC	60 °C
E-cadherin	Sense: TAC GCC TGG GAC TCC ACC TA Anti-sense: CCA GAA ACG GAG GCC TGA T	60 °C
GAPDH	Sense: AGGCTGTTGTCATACTTCTCAT Anti-sense: GGAGTCCACTGGCGTCTT	60 °C

dry milk /TBS-T for 1 h at room temperature. Subsequently, the membranes were washed three times for 5 min with TBS-T and detection of the proteins was performed with ECL (#WBKLS0500, Immobilon™ Western Chemiluminescent HRP Substrate, Millipore), according to the manufacturer's instructions.

Molecular size analysis of hyaluronan in supernatants of MDA-MB-231 breast cancer cells

Analysis of the size of hyaluronan in the cultured media of MDA-MB-231 cells was performed by agarose gel electrophoresis as described in the online protocol (PEGNAC_HA_Size; NHLB1 award number PO1HL107147). Briefly, 60×10^4 cells were seeded in 60 mm dishes, cultured with complete medium for 24 h and starved overnight (16-18 h) with serum free culture media. Then, cells were treated with 10 mM salicylate in the absence (0%) of serum for 24 h and the supernatants were collected. The conditioned medium was incubated with 0.1 µg/mL Proteinase K (Ambion, Cat. No. #AM2546) at 60 °C for 4 h. Then, 4 volumes of pre-chilled (–20 °C) 100% ethanol were added to each sample followed by incubation at –20 °C, overnight. Next, the samples were centrifuged at 4,000 RPM for 10 min, at room temperature and the supernatants were discarded. The pellets were washed by adding 1 mL of pre-chilled (–20 °C) 75% ethanol, vortexing and centrifugation at 13,000 RPM for 10 min, at room temperature. The supernatants were discarded, residual ethanol was removed with pipette and the samples were air-dried for 20 min at room temperature. The pellets where then diluted in 200 µL of 100 mM ammonium acetate by vortexing followed by incubation at room temperature for 20 min. Next, the proteinase K was heat inactivated at 100 °C for 5 min. Samples were left on ice to chill for 5 min and the nucleic acids were digested with 25 U/µL DNase at 37 °C, overnight. The next day, the enzyme was heat inactivated at 95 °C for 5 min. Afterwards, 400 µL of pre-chilled (–20 °C) 100% ethanol were added to each sample and incubated overnight at –20 °C. The samples were then centrifuged at 13,000 RPM for 10 min at room temperature and the supernatants were discarded. The pellets were washed with 1 mL of pre-chilled (–20 °C) 75% ethanol, vortexed and centrifuged at 13,000 RPM for 10 min. The supernatants were once more discarded, residual ethanol was removed with pipette and the pellets were air-dried for 20 min. The pellets were re-suspended in 100 µL of 100 mM ammonium acetate and lyophilized in centrifugal vacuum concentrator, re-suspended in 15 µL of 10 M formamide and left overnight at 4 °C. Then, 0.2 µL of sample loading buffer (0.2% bromophenol blue in 10 M formamide) per 10 µL of sample were added and the samples were loaded in 2% agarose gel (SeaKem GTG agarose, made with TAE buffer). Electrophoresis was run for 45 min at 100 V. Hyaluronan standard (1000 kDa, Q-Med, Uppsala, Sweden) was run in parallel. The gel was then equilibrated for 1 h in 30% ethanol and incubated with Stains-All solution (Sigma, Cat. No. #E9379, final concentration 25 µg/mL) in 30% ethanol in dH_2O. After overnight incubation at room temperature in the dark, the staining solution was discarded and replaced by dH_2O for 1 h to destain. The gel was scanned using an Epson scanner.

Statistical analysis

Each experiment was performed at least three times. Reported values are expressed as mean ± standard deviation. Significance in experiments with two groups were determined by unpaired Student's *t*-test, whereas statistical analyses for experiments with more than two groups were calculated via One-way analysis of variance (ANOVA) (*p<0.05, **p<0.01, ***p <0.001, $^{\#}$p<0.001).

Acknowledgments

This research was supported by Grant (project code: 80626) from the Research Committee of the University of Patras, Greece, via "C. CARATHEODORI" program and co-financed by Greece and the European Union (European Social Fund-ESF) through the Operational Programme "Human Resources Development, Education and Lifelong Learning" in the context of the project "Strengthening Human Resources Research Potential via Doctorate Research – 2nd Cycle" (MIS-5000432), implemented by the State Scholarships Foundation (IKY).

Declaration of competing interest

The authors declare that they have no conflict of interest.

Appendix A. Supplementary data

Supplementary data to this article can be found online at https://doi.org/10.1016/j.mbplus.2020.100031.

Received 23 November 2019;
Received in revised form 25 February 2020;
Accepted 26 February 2020
Available online 5 March 2020

Keywords:
Hyaluronan;
CD44;
Hyaluronan synthase 2;
AMPK;
Salicylate;
Aspirin;
Breast cancer

References

[1] C.M. Perou, T. Sorlie, M.B. Eisen, M. van de Rijn, S.S. Jeffrey, C.A. Rees, J.R. Pollack, D.T. Ross, H. Johnsen, L.A. Akslen, O. Fluge, A. Pergamenschikov, C. Williams, S.X. Zhu, P.E. Lonning, A.L. Borresen-Dale, P.O. Brown, D. Botstein, Molecular portraits of human breast tumours, Nature 406 (2000) 747–752.

[2] P. Heldin, K. Basu, I. Kozlova, H. Porsch, HAS2 and CD44 in breast tumorigenesis, Adv. Cancer Res. 123 (2014) 211–229.

[3] P. Auvinen, R. Tammi, J. Parkkinen, M. Tammi, U. Agren, R. Johansson, P. Hirvikoski, M. Eskelinen, V.M. Kosma, Hyaluronan in peritumoral stroma and malignant cells associates with breast cancer spreading and predicts survival, Am. J. Pathol. 156 (2000) 529–536.

[4] P. Heldin, C.Y. Lin, C. Kolliopoulos, Y.H. Chen, S.S. Skandalis, Regulation of hyaluronan biosynthesis and clinical impact of excessive hyaluronan production, Matrix Biol. 78-79 (2019) 100–117.

[5] T.C. Laurent, J.R. Fraser, Hyaluronan, FASEB journal : official publication of the Federation of American Societies for Experimental Biology 6 (1992) 2397–2404.

[6] E. Karousou, S. Misra, S. Ghatak, K. Dobra, M. Gotte, D. Vigetti, A. Passi, N.K. Karamanos, S.S. Skandalis, Roles and targeting of the HAS/hyaluronan/CD44 molecular system in cancer, Matrix Biol. 59 (2017) 3–22.

[7] V.C. Hascall, A.K. Majors, C.A. De La Motte, S.P. Evanko, A. Wang, J.A. Drazba, S.A. Strong, T.N. Wight, Intracellular hyaluronan: a new frontier for inflammation? Biochim. Biophys. Acta 1673 (2004) 3–12.

[8] S.S. Skandalis, T. Karalis, P. Heldin, Intracellular hyaluronan: importance for cellular functions, Seminars in cancer biology In Press 62 (2020) 20–30.

[9] H. Ponta, L. Sherman, P.A. Herrlich, CD44: from adhesion molecules to signalling regulators, Nat Rev Mol Cell Biol 4 (2003) 33–45.

[10] S. Misra, P. Heldin, V.C. Hascall, N.K. Karamanos, S.S. Skandalis, R.R. Markwald, S. Ghatak, Hyaluronan-CD44 interactions as potential targets for cancer therapy, FEBS J. 278 (2011) 1429–1443.

[11] K. Kouvidi, A. Berdiaki, D. Nikitovic, P. Katonis, N. Afratis, V. C. Hascall, N.K. Karamanos, G.N. Tzanakakis, Role of receptor for hyaluronic acid-mediated motility (RHAMM) in low molecular weight hyaluronan (LMWHA)-mediated fibrosarcoma cell adhesion, J. Biol. Chem. 286 (2011) 38509–38520.

[12] D. Jiang, J. Liang, P.W. Noble, Hyaluronan as an immune regulator in human diseases, Physiol. Rev. 91 (2011) 221–264.

[13] R.M. Tighe, S. Garantziotis, Hyaluronan interactions with innate immunity in lung biology, Matrix Biol. 78-79 (2019) 84–99.

[14] N.K. Karamanos, A.D. Theocharis, T. Neill, R.V. Iozzo, Matrix modeling and remodeling: a biological interplay regulating tissue homeostasis and diseases, Matrix Biol. 75-76 (2019) 1–11.

[15] S.S. Skandalis, T.T. Karalis, A. Chatzopoulos, N.K. Karamanos, Hyaluronan-CD44 axis orchestrates cancer stem cell functions, Cell. Signal. 63 (2019) 109377.

[16] T.C. Laurent, U.B. Laurent, J.R. Fraser, The structure and function of hyaluronan: an overview, Immunol. Cell Biol. 74 (1996) A1–A7.

[17] M.I. Tammi, S. Oikari, S. Pasonen-Seppanen, K. Rilla, P. Auvinen, R.H. Tammi, Activated hyaluronan metabolism in the tumor matrix - causes and consequences, Matrix Biol. 78-79 (2019) 147–164.

[18] S. Garantziotis, R.C. Savani, Hyaluronan biology: a complex balancing act of structure, function, location and context, Matrix Biol. 78-79 (2019) 1–10.

[19] A. Jacobson, J. Brinck, M.J. Briskin, A.P. Spicer, P. Heldin, Expression of human hyaluronan synthases in response to external stimuli, Biochem. J. 348 (Pt 1) (2000) 29–35.
[20] C. Kolliopoulos, C.Y. Lin, C.H. Heldin, A. Moustakas, P. Heldin, Has2 natural antisense RNA and Hmga2 promote Has2 expression during TGFbeta-induced EMT in breast cancer, Matrix Biol. 80 (2019) 29–45.
[21] D. Vigetti, E. Karousou, M. Viola, S. Deleonibus, G. De Luca, A. Passi, Hyaluronan: biosynthesis and signaling, Biochim. Biophys. Acta 1840 (2014) 2452–2459.
[22] D. Vigetti, M. Viola, E. Karousou, G. De Luca, A. Passi, Metabolic control of hyaluronan synthases, Matrix Biol. 35 (2014) 8–13.
[23] A.J. Deen, U.T. Arasu, S. Pasonen-Seppanen, A. Hassinen, P. Takabe, S. Wojciechowski, R. Karna, K. Rilla, S. Kellokumpu, R. Tammi, M. Tammi, S. Oikari, UDP-sugar substrates of HAS3 regulate its O-GlcNAcylation, intracellular traffic, extracellular shedding and correlate with melanoma progression, Cellular and molecular life sciences : CMLS 73 (2016) 3183–3204.
[24] S. Oikari, T. Kettunen, S. Tiainen, J. Hayrinen, A. Masarwah, M. Sudah, A. Sutela, R. Vanninen, M. Tammi, P. Auvinen, UDP-sugar accumulation drives hyaluronan synthesis in breast cancer, Matrix Biol. 67 (2018) 63–74.
[25] E. Karousou, M. Kamiryo, S.S. Skandalis, A. Ruusala, T. Asteriou, A. Passi, H. Yamashita, U. Hellman, C.H. Heldin, P. Heldin, The activity of hyaluronan synthase 2 is regulated by dimerization and ubiquitination, J. Biol. Chem. 285 (2010) 23647–23654.
[26] D. Vigetti, S. Deleonibus, P. Moretto, E. Karousou, M. Viola, B. Bartolini, V.C. Hascall, M. Tammi, G. De Luca, A. Passi, Role of UDP-N-acetylglucosamine (GlcNAc) and O-GlcNAcylation of hyaluronan synthase 2 in the control of chondroitin sulfate and hyaluronan synthesis, J. Biol. Chem. 287 (2012) 35544–35555.
[27] D. Vigetti, M. Clerici, S. Deleonibus, E. Karousou, M. Viola, P. Moretto, P. Heldin, V.C. Hascall, G. De Luca, A. Passi, Hyaluronan synthesis is inhibited by adenosine monophosphate-activated protein kinase through the regulation of HAS2 activity in human aortic smooth muscle cells, J. Biol. Chem. 286 (2011) 7917–7924.
[28] G.R. Steinberg, B.E. Kemp, AMPK in health and disease, Physiol. Rev. 89 (2009) 1025–1078.
[29] M.C. Towler, D.G. Hardie, AMP-activated protein kinase in metabolic control and insulin signaling, Circ. Res. 100 (2007) 328–341.
[30] J. Cuzick, F. Otto, J.A. Baron, P.H. Brown, J. Burn, P. Greenwald, J. Jankowski, C. La Vecchia, F. Meyskens, H.J. Senn, M. Thun, Aspirin and non-steroidal anti-inflammatory drugs for cancer prevention: an international consensus statement, The Lancet. Oncology 10 (2009) 501–507.
[31] P.M. Rothwell, M. Wilson, C.E. Elwin, B. Norrving, A. Algra, C.P. Warlow, T.W. Meade, Long-term effect of aspirin on colorectal cancer incidence and mortality: 20-year follow-up of five randomised trials, Lancet 376 (2010) 1741–1750.
[32] P.M. Rothwell, M. Wilson, J.F. Price, J.F. Belch, T.W. Meade, Z. Mehta, Effect of daily aspirin on risk of cancer metastasis: a study of incident cancers during randomised controlled trials, Lancet 379 (2012) 1591–1601.
[33] H. Hua, H. Zhang, Q. Kong, J. Wang, Y. Jiang, Complex roles of the old drug aspirin in cancer chemoprevention and therapy, Med. Res. Rev. 39 (2019) 114–145.
[34] G.A. Higgs, J.A. Salmon, B. Henderson, J.R. Vane, Pharmacokinetics of aspirin and salicylate in relation to inhibition of arachidonate cyclooxygenase and antiinflammatory activity, Proc. Natl. Acad. Sci. U. S. A. 84 (1987) 1417–1420.
[35] F.M. Williams, Clinical significance of esterases in man, Clin. Pharmacokinet. 10 (1985) 392–403.
[36] T.D. Warner, F. Giuliano, I. Vojnovic, A. Bukasa, J.A. Mitchell, J.R. Vane, Nonsteroid drug selectivities for cyclo-oxygenase-1 rather than cyclo-oxygenase-2 are associated with human gastrointestinal toxicity: a full in vitro analysis, Proc. Natl. Acad. Sci. U. S. A. 96 (1999) 7563–7568.
[37] X.M. Xu, L. Sansores-Garcia, X.M. Chen, N. Matijevic-Aleksic, M. Du, K.K. Wu, Suppression of inducible cyclooxygenase 2 gene transcription by aspirin and sodium salicylate, Proc. Natl. Acad. Sci. U. S. A. 96 (1999) 5292–5297.
[38] K. Shirakawa, L. Wang, N. Man, J. Maksimoska, A.W. Sorum, H.W. Lim, I.S. Lee, T. Shimazu, J.C. Newman, S. Schroder, M. Ott, R. Marmorstein, J. Meier, S. Nimer, E. Verdin, Salicylate, diflunisal and their metabolites inhibit CBP/p300 and exhibit anticancer activity, eLife 5 (2016), e11156.
[39] P. Boueroy, R. Aukkanimart, T. Boonmars, P. Sriraj, P. Ratanasuwan, A. Juasook, N. Wonkchalee, K. Vaeteewoottacharn, S. Wongkham, Inhibitory effect of aspirin on cholangiocarcinoma cells, Asian Pacific journal of cancer prevention : APJCP 18 (2017) 3091–3096.
[40] X. Dai, J. Yan, X. Fu, Q. Pan, D. Sun, Y. Xu, J. Wang, L. Nie, L. Tong, A. Shen, M. Zheng, M. Huang, M. Tan, H. Liu, X. Huang, J. Ding, M. Geng, Aspirin inhibits cancer metastasis and angiogenesis via targeting heparanase, Clinical cancer research : an official journal of the American Association for Cancer Research 23 (2017) 6267–6278.
[41] J. Madunic, L. Horvat, I. Majstorovic, I. Jodlowska, M. Antica, M. Matulic, Sodium salicylate inhibits urokinase activity in MDA MB-231 breast cancer cells, Clinical breast cancer 17 (2017) 629–637.
[42] S.A. Hawley, M.D. Fullerton, F.A. Ross, J.D. Schertzer, C. Chevtzoff, K.J. Walker, M.W. Peggie, D. Zibrova, K.A. Green, K.J. Mustard, B.E. Kemp, K. Sakamoto, G.R. Steinberg, D.G. Hardie, The ancient drug salicylate directly activates AMP-activated protein kinase, Science 336 (2012) 918–922.
[43] N.K. Karamanos, Z. Piperigkou, A.D. Theocharis, H. Watanabe, M. Franchi, S. Baud, S. Brezillon, M. Gotte, A. Passi, D. Vigetti, S. Ricard-Blum, R.D. Sanderson, T. Neill, R.V. Iozzo, Proteoglycan chemical diversity drives multifunctional cell regulation and therapeutics, Chem. Rev. 118 (2018) 9152–9232.
[44] P. Auvinen, K. Rilla, R. Tumelius, M. Tammi, R. Sironen, Y. Soini, V.M. Kosma, A. Mannermaa, J. Viikari, R. Tammi, Hyaluronan synthases (HAS1-3) in stromal and malignant cells correlate with breast cancer grade and predict patient survival, Breast Cancer Res. Treat. 143 (2014) 277–286.
[45] L. Udabage, G.R. Brownlee, M. Waltham, T. Blick, E.C. Walker, P. Heldin, S.K. Nilsson, E.W. Thompson, T.J. Brown, Antisense-mediated suppression of hyaluronan synthase 2 inhibits the tumorigenesis and progression of breast cancer, Cancer Res. 65 (2005) 6139–6150.
[46] Y. Li, L. Li, T.J. Brown, P. Heldin, Silencing of hyaluronan synthase 2 suppresses the malignant phenotype of invasive breast cancer cells, Int. J. Cancer 120 (2007) 2557–2567.
[47] T.T. Karalis, P. Heldin, D.H. Vynios, T. Neill, S. Buraschi, R. V. Iozzo, N.K. Karamanos, S.S. Skandalis, Tumor-suppressive functions of 4-MU on breast cancer cells of different ER status: regulation of hyaluronan/HAS2/CD44

and specific matrix effectors, Matrix Biol. 78-79 (2019) 118–138.
[48] G.A. Higgs, S. Moncada, J.R. Vane, Eicosanoids in inflammation, Ann. Clin. Res. 16 (1984) 287–299.
[49] M. Yuan, N. Konstantopoulos, J. Lee, L. Hansen, Z.W. Li, M. Karin, S.E. Shoelson, Reversal of obesity- and diet-induced insulin resistance with salicylates or targeted disruption of Ikkbeta, Science 293 (2001) 1673–1677.
[50] F.V. Din, A. Valanciute, V.P. Houde, D. Zibrova, K.A. Green, K. Sakamoto, D.R. Alessi, M.G. Dunlop, Aspirin inhibits mTOR signaling, activates AMP-activated protein kinase, and induces autophagy in colorectal cancer cells, Gastroenterology 142 (2012) 1504–1515(e1503).
[51] M.G. Luciani, C. Campregher, C. Gasche, Aspirin blocks proliferation in colon cells by inducing a G1 arrest and apoptosis through activation of the checkpoint kinase ATM, Carcinogenesis 28 (2007) 2207–2217.
[52] Y. He, H. Huang, C. Farischon, D. Li, Z. Du, K. Zhang, X. Zheng, S. Goodin, Combined effects of atorvastatin and aspirin on growth and apoptosis in human prostate cancer cells, Oncol. Rep. 37 (2017) 953–960.
[53] D. Liao, L. Zhong, T. Duan, R.H. Zhang, X. Wang, G. Wang, K. Hu, X. Lv, T. Kang, Aspirin suppresses the growth and metastasis of osteosarcoma through the NF-kappaB pathway, Clinical cancer research : an official journal of the American Association for Cancer Research 21 (2015) 5349–5359.
[54] Y. Huang, L.M. Lichtenberger, M. Taylor, J.N. Bottsford-Miller, M. Haemmerle, M.J. Wagner, Y. Lyons, S. Pradeep, W. Hu, R.A. Previs, J.M. Hansen, D. Fang, P.L. Dorniak, J. Filant, E.J. Dial, F. Shen, H. Hatakeyama, A.K. Sood, Antitumor and antiangiogenic effects of aspirin-PC in ovarian cancer, Mol. Cancer Ther. 15 (2016) 2894–2904.
[55] C.G. Chen, M.A. Gubbiotti, A. Kapoor, X. Han, Y. Yu, R.J. Linhardt, R.V. Iozzo, Autophagic degradation of HAS2 in endothelial cells: a novel mechanism to regulate angiogenesis, Matrix Biol In Press (2020).
[56] G. Levy, T. Tsuchiya, Salicylate accumulation kinetics in man, N. Engl. J. Med. 287 (1972) 430–432.
[57] S. Redondo, C.G. Santos-Gallego, P. Ganado, M. Garcia, L. Rico, M. Del Rio, T. Tejerina, Acetylsalicylic acid inhibits cell proliferation by involving transforming growth factor-beta, Circulation 107 (2003) 626–629.
[58] S.J. Shiff, M.I. Koutsos, L. Qiao, B. Rigas, Nonsteroidal antiinflammatory drugs inhibit the proliferation of colon adenocarcinoma cells: effects on cell cycle and apoptosis, Exp. Cell Res. 222 (1996) 179–188.
[59] R. Cheng, Y.J. Liu, J.W. Cui, M. Yang, X.L. Liu, P. Li, Z. Wang, L.Z. Zhu, S.Y. Lu, L. Zou, X.Q. Wu, Y.X. Li, Y. Zhou, Z. Y. Fang, W. Wei, Aspirin regulation of c-myc and cyclinD1 proteins to overcome tamoxifen resistance in estrogen receptor-positive breast cancer cells, Oncotarget 8 (2017) 30252–30264.
[60] F.V. Din, M.G. Dunlop, L.A. Stark, Evidence for colorectal cancer cell specificity of aspirin effects on NF kappa B signalling and apoptosis, Br. J. Cancer 91 (2004) 381–388.
[61] J.L. Lee, M.J. Wang, J.Y. Chen, Acetylation and activation of STAT3 mediated by nuclear translocation of CD44, J. Cell Biol. 185 (2009) 949–957.
[62] S.P. Evanko, T.N. Wight, Intracellular localization of hyaluronan in proliferating cells, J. Histochem. Cytochem. 47 (1999) 1331–1342.
[63] B.P. Toole, Hyaluronan: from extracellular glue to pericellular cue, Nat. Rev. Cancer 4 (2004) 528–539.
[64] M. Banys-Paluchowski, I. Witzel, B. Aktas, P.A. Fasching, A. Hartkopf, W. Janni, S. Kasimir-Bauer, K. Pantel, G. Schon, B. Rack, S. Riethdorf, E.F. Solomayer, T. Fehm, V. Muller, The prognostic relevance of urokinase-type plasminogen activator (uPA) in the blood of patients with metastatic breast cancer, Sci. Rep. 9 (2019) 2318.
[65] R. Wu, A.L. Abramson, M.J. Shikowitz, A.J. Dannenberg, B. M. Steinberg, Epidermal growth factor-induced cyclooxygenase-2 expression is mediated through phosphatidylinositol-3 kinase, not mitogen-activated protein/extracellular signal-regulated kinase kinase, in recurrent respiratory papillomas, Clinical cancer research : an official journal of the American Association for Cancer Research 11 (2005) 6155–6161.
[66] S.S. Qadri, J.H. Wang, K.C. Redmond, O.D. AF, T. Aherne, H.P. Redmond, The role of COX-2 inhibitors in lung cancer, Ann. Thorac. Surg. 74 (2002) 1648–1652.
[67] M. Lu, A. Strohecker, F. Chen, T. Kwan, J. Bosman, V.C. Jordan, V.L. Cryns, Aspirin sensitizes cancer cells to TRAIL-induced apoptosis by reducing survivin levels, Clinical cancer research : an official journal of the American Association for Cancer Research 14 (2008) 3168–3176.
[68] S. Misra, L.M. Obeid, Y.A. Hannun, S. Minamisawa, F.G. Berger, R.R. Markwald, B.P. Toole, S. Ghatak, Hyaluronan constitutively regulates activation of COX-2-mediated cell survival activity in intestinal epithelial and colon carcinoma cells, J. Biol. Chem. 283 (2008) 14335–14344.
[69] U.C. Mc Menamin, C.R. Cardwell, C.M. Hughes, L.J. Murray, Low-dose aspirin use and survival in breast cancer patients: a nationwide cohort study, Cancer Epidemiol. 47 (2017) 20–27.
[70] M. Feoktistova, P. Geserick, M. Leverkus, Crystal Violet Assay for Determining Viability of Cultured Cells, 2016 Cold Spring Harbor Protocols, 2016 (pdb prot087379).